HHS Public Access

Author manuscript

Cortex. Author manuscript; available in PMC 2016 December 01.

Published in final edited form as:

Cortex. 2015 December ; 73: 203–215. doi:10.1016/j.cortex.2015.09.005.

PREDICTING APHASIA TYPE FROM BRAIN DAMAGE MEASURED WITH STRUCTURAL MRI

Grigori Yourganov[a,*], **Kimberly G. Smith**[b], **Julius Fridriksson**[b], and **Chris Rorden**[a]

[a]Department of Psychology, University of South Carolina, Columbia, SC, 29208, USA

[b]Department of Communication Sciences and Disorders, University of South Carolina, Columbia, SC, 29208, USA

Abstract

Chronic aphasia is a common consequence of a left-hemisphere stroke. Since the early insights by Broca and Wernicke, studying the relationship between the loci of cortical damage and patterns of language impairment has been one of the concerns of aphasiology. We utilized multivariate classification in a cross-validation framework to predict the type of chronic aphasia from the spatial pattern of brain damage. Our sample consisted of 98 patients with five types of aphasia (Broca's, Wernicke's, global, conduction, and anomic), classified based on scores on the Western Aphasia Battery. Binary lesion maps were obtained from structural MRI scans (obtained at least 6 months poststroke, and within 2 days of behavioural assessment); after spatial normalization, the lesions were parcellated into a disjoint set of brain areas. The proportion of damage to the brain areas was used to classify patients' aphasia type. To create this parcellation, we relied on five brain atlases; our classifier (support vector machine) could differentiate between different kinds of aphasia using any of the five parcellations. In our sample, the best classification accuracy was obtained when using a novel parcellation that combined two previously published brain atlases, with the first atlas providing the segmentation of grey matter, and the second atlas used to segment the white matter. For each aphasia type, we computed the relative importance of different brain areas for distinguishing it from other aphasia types; our findings were consistent with previously published reports of lesion locations implicated in different types of aphasia. Overall, our results revealed that automated multivariate classification could distinguish between aphasia types based on damage to atlas-defined brain areas.

Keywords

chronic aphasia; aphasia typology; multivariate classification

[*]Corresponding author: Phone: +1 803 369 5797, yourgano@musc.edu, Address: Department of Psychology, University of South Carolina, 1512 Pendleton Street, Columbia, SC 29208, USA. Present address: Department of Neurology, Medical University of South Carolina, 171 Ashley Avenue, Charleston, SC 29425, USA.

1. INTRODUCTION

Aphasia is a language disorder frequently observed after damage to the left hemisphere of the brain. Depending on the location of damage in relation to the cortical language regions, aphasic patients can demonstrate very different patterns of language impairment. In general, patients with similar lesion location and size show somewhat similar aphasic symptoms. Nevertheless, there is a fair amount of heterogeneity in patterns of cortical damage across patients with similar language impairments (Willmes & Poeck, 1993). Such heterogeneity is expected in clinical populations; however, when this variance is too great it suggests that group studies might be "useless and harmful" for understanding individual symptoms (Caramazza & McCloskey, 1988). On the other hand, it is possible that the relationship between symptoms and structural injury reflect specific patterns of injury to a spatially distributed network; in this case, multivariate analysis is more sensitive than the more traditional univariate approaches that ignore the interactions between spatial locations (see e.g. Yourganov et al., 2014). Our objective was to determine whether automated multivariate classification algorithms could accurately predict aphasia type based on the pattern of brain injury.

Modern aphasia classification largely rests on a model of language localization typically referred to as the Wernicke-Lichtheim model. This model was largely developed by Wernicke and Lichtheim between 1874 and 1886 (for a comprehensive historical account and bibliography, see Tesak & Code, 2008), and brought together previous and concurrent ideas about language localization (notably, Dax's insight on the connection between left-hemisphere lesions and speech disorders; Broca's pioneering results on the localization of the motor centre within the inferior frontal lobe; Meynert's idea of the importance of the peri-Sylvian region in speech comprehension; Kussmaul's hypothesis of a concept center in the brain, although Kussmaul did not hypothesize its specific location). The Wernicke-Lichtheim model postulates the existence of three interconnected "language centers": sensory, motor, and concept (the original Wernicke's model consisted of only the sensory and motor centers; Lichtheim added the concept center, without specifying its anatomical location; Wernicke revised his model accordingly). Damage to each center and connective tract would result in a specific aphasia type, with the exception of damage to the concept center, which would cause memory deficits rather than aphasia. According to this model, damage to the motor and sensory centers produces impairment in expression and comprehension, respectively called motor and sensory aphasia. Damage to the tract that connects these two centers, the arcuate fasciculus, results in conduction aphasia, which manifests in difficulties repeating others' speech. When the connections between these two centers and the concept center are damaged, it results in two forms of transcortical aphasia (Tesak & Code, 2008, p.90–91): transcortical motor aphasia, in which a patient has difficulty with expression but repetition is relatively preserved, and transcortical sensory aphasia, in which comprehension is impaired, but repetition is preserved. When the damage is extensive and covers several loci, it results in what Lichtheim called total aphasia (Lichtheim, 1885); a condition that today is typically referred to as global aphasia. Finally, amnestic aphasia (now more commonly referred to as 'anomic aphasia') is a relatively mild language impairment manifested in word-finding difficulties; it is not linked to damage to a

specific locus. This model of language localization revolutionized the concept of aphasia typology despite resistance from others in the field.

These early accounts provided the basis for Norman Geschwind's seminal writings on the classification of aphasia and associated lesion locations (Geschwind & Kaplan, 1962; Geschwind, 1965; Geschwind & Fusillo, 1966). He proposed the concept of cortical disconnection. Specifically, a brain lesion could affect either a discrete cortical area, the connecting fibers between these areas, or both. The symptoms of aphasia were based on the specific location of the lesion. Geschwind's proposal remains relevant today, as researchers utilize new neuroimaging techniques to provide a more precise account of the anatomical substrate underlying language dysfunction and informing classification of aphasia syndromes (Benson & Ardila, 1996). Although classification of aphasia based on clusters of symptoms has been criticized on the premise that no two individuals with aphasia present with the same clinical symptoms (Caplan, 1987; Carmazza, 1984; Schwartz, 1984), syndrome classification, while limiting at times, has remained fairly consistent and replicable for over a century.

These historical accounts of aphasia classification form the basis for modern aphasia typology and the foundation to current aphasia classification systems. Most aphasia typology schemes include such types as Broca's, Wernicke's, conduction, transcortical motor and sensory, anomic, and global aphasia (Ardila, 2010). A notable exception is the system proposed by Luria (1970), with a markedly different definition of aphasia types (it should be noted that Luria investigated aphasia in patients suffering from bullet wounds, rather than from stroke-related lesions). The type of aphasia is now commonly determined based on standardized behavioural testing; for example, the Western Aphasia Battery (WAB; Kertesz, 1982; Kertesz, 2006) was developed with the explicit purpose relating patterns of language impairment to a particular classical aphasia type.

The aphasia syndromes and associated clinical symptoms are constrained by the underlying vasculature. In fact, Hillis discussed the classic aphasia typology as vascular syndromes "consisting of frequently associated deficits that reflect damage or dysfunction of regions of neural tissue (essential for particular language functions) supplied by a particular artery" (Hillis, 2007). Damage to brain regions supplied by the superior division of the middle cerebral artery (MCA), such as the left posterior inferior frontal cortex and insula, result in Broca's aphasia symptomatology (e.g., non-fluent speech production, relatively spared auditory comprehension, and, in some cases, agrammatic sentence processing). Deficits associated with Wernicke's aphasia (e.g., fluent jargon and poor auditory comprehension) are typically related to damage of neural regions supplied by the inferior division of the left MCA. Transcortical motor aphasia is thought to be caused by damage to brain regions supplied by the anterior cerebral artery (ACA; Masdeu et al., 1979; Rubens, 1976) or watershed regions between the ACA and MCA (Hillis, 2007), with lesions occurring anterior and superior to Broca's area (Freedman et al., 1984). Lesions to regions around Wernicke's area that are supplied by the posterior cerebral artery (PCA) and watershed areas between the MCA and PCA territory (Alexander et al., 1989) result in symptoms associated with transcortical sensory aphasia. Global aphasia is associated with extensive cortical damage in the region supplied by the MCA; in most cases, both Broca's area and

Wernicke's area are damaged (Mazzocchi & Vignolo, 1979). Conduction aphasia, characterized by good comprehension, frequent phonemic errors in speech production and poor repetition, has historically been associated with lesions of the arcuate fasciculus, a white-matter tract connecting Broca's and Wernicke's areas (Geschwind, 1965). However, more recent evidence indicates this syndrome is related to lesions of the supramarginal gyrus, left dorsal superior temporal gyrus, or the temporo-parietal junction (Buchsbaum et al., 2011; Hickok et al., 2000; Anderson et al., 1999; Palumbo et al., 1992; Selnes et al., 1992; Damasio & Damasio, 1980).

Classification of aphasia syndromes has proven useful in both clinical and research settings. It remains common to report aphasia types in clinical studies of aphasia because it is expected that patients with the same aphasia type present with similar clinical symptoms and patterns of brain damage. In addition, it is expected that research and clinical findings are potentially applicable to patients with a similar cluster of symptoms. Classification has allowed clinicians to predict recovery (Kertesz, 1997) and to select patients for appropriate interventions (Chapey, 2001). Importantly, aphasia syndromes classified based on clinical assessment has allowed clinicians to make robust predictions about the areas of the brain that are damaged, and in particular, hypoperfused (Hillis, 2007). Reineck and colleagues (2005) examined how assessment of language function can be useful acutely to estimate the site and volume of hypoperfusion in patients with aphasia, and in conjunction with diffusion weighted imaging, identify patients who might benefit from reperfusion therapy and possibly predict prognosis (Reineck & Hillis, 2004; Reineck et al., 2005).

With the accumulation of neurological findings, determination of aphasia type from brain damage has become less clear than the classical Wernicke-Lichtheim model had suggested. As mentioned above, conduction aphasia is now considered a result of damage to grey matter around the temporo-parietal junction (Damasio, 1982; Hickok et al., 2000), rather than exclusively white-matter damage (i.e., arcuate fasciculus) as proposed by the classical Wernicke-Lichtheim model. The damage limited to Broca's area does not lead to Broca's aphasia, and the same can be said about Wernicke's area and Wernicke's aphasia (Damasio, 1982, Fridriksson et al., 2014). Early attempts to predict aphasia type from brain damage (Basso et al., 1985; Willmes & Poeck, 1993) have reported poor prediction accuracies. This is likely caused by the heterogeneity of brain damage within groups of the same aphasia type. Over time, larger sample sizes and better imaging techniques led to a more accurate localization of aphasia symptoms (Kreisler et al., 2000; Henseler et al., 2013). However, the most common approach to studying the neurological causes of aphasia is voxel-based lesion-symptom mapping (Bates et al., 2003), which is a univariate method where the impact of each cortical location is evaluated independent of the other locations; this might introduce a spatial bias, as reported by Mah et al. (2014).

An alternative (multivariate) approach has recently gained popularity in neuroimaging studies (see, for example, Pereira et al., 2009). This approach evaluates the contribution of all brain locations (which could be voxels or cortical regions) at once; the interactions between the locations are considered as important as the contributions of each specific location. It is relevant to stroke studies because stroke usually damages multiple brain areas. Schmah and colleagues (2010) analyzed fMRI data from a longitudinal stroke study using

several multivariate and univariate algorithms, and evaluated the algorithms on their ability to predict the post-stroke onset and the task (e.g., finger tapping versus wrist flexion). Saur and colleagues (2010) used a multivariate method called Support Vector Machine (SVM) to predict the post-stroke recovery of function. Smith et al. (2013) used SVM to diagnose acute spatial neglect. In the current study, we used SVM to predict aphasia type based on patterns of brain damage. To our knowledge, this is the first study to classify aphasia using a multivariate approach, although the multivariate framework has been applied to the diagnosis of such neurological disorders as dementia, schizophrenia and Parkinson's disease (Orru et al., 2012).

The three main components of our approach are: (1) careful spatial normalization of lesions; (2) segmentation of the lesioned area using a brain atlas; (3) multivariate prediction of aphasia type within a cross-validation framework. The goal of the first step is to lessen the impact of individual differences in cortical shape and size; for this purpose, we adapted our Clinical Toolbox (Rorden et al., 2012) to support enantiomorphic normalization (Nachev et al., 2008) using SPM12. The second step serves to reduce the number of inputs to the multivariate analysis. These inputs are called *features* in the machine learning literature (Pereira et al. 2010), and the stability of predictions is often impaired by using a large number of features. In our analysis, we used a brain atlas (e.g., the Brodmann atlas) to define the brain areas and to compute the amount of damage to each area; the left-hemisphere areas are the features for our predictive algorithm. This step transforms a large number of binary features (voxels, which are either damaged or not) into a much smaller set of continuous-valued features (brain areas with an associated proportion of damage). The atlas-based approach, combined with multivariate analysis that accounts for simultaneous contribution of different brain areas to a given behavioural syndrome, has the potential to diminish the spatial bias that was reported by Mah et al. (2014), although it does not eliminate the bias completely (that would require functionally homogeneous brain areas, where the relationship between the damage and behavioural deficit is uniform across areas). The downside of the atlas-based approach is relatively poorer spatial localization because our spatial resolution is defined by brain areas rather than by voxels. For our purpose, a brain atlas is efficient if it segments the brain into the areas such that aphasia type can be decoded from damage to these areas. Lastly, during the third step, SVM estimates the association between patterns of brain damage and aphasia types ("training"), and assigns the type to previously unseen patients based on their pattern of brain damage ("testing").

Our cohort is a group of 98 chronic stroke patients with aphasia. We used multivariate classification to distinguish between five aphasia types: Broca's, Wernicke's, anomic, global, and conduction. Unfortunately, our sample did not have any patients with transcortical sensory aphasia and only one patient with transcortical motor aphasia, who had to be excluded because we needed the absolute minimum of two representatives of each aphasia type (one used for training and another for testing). Lesions were defined from the structural MRI scans by a neurologist. To segment the lesions, we used a set of brain atlases, some containing only white or only grey matter areas, and some containing both. Our study shows that, despite patient heterogeneity, there is a correspondence between the spatial pattern of brain damage and the resulting language deficit, which has significant

implications for diagnosis, prognosis, and therapeutic intervention for the recovery of language in individuals with aphasia.

2. MATERIALS AND METHODS

2.1 Participants

Our participant sample was selected from 139 right-handed patients with chronic left hemisphere stroke. Recruitment relied on referrals from local neurologists and advertisements in print and radio media in the state of South Carolina; the study was approved by the local ethics committee. The behavioural assessment of the patients took place between May 2007 and October 2014. Out of these patients, 98 persons were included in the current study. The exclusion criteria were: absence of aphasia (n=19); MRI scanning could not be performed for health concerns (n=15); speech deficits were driven by apraxia of speech rather than aphasia (n=2); the stroke lesion was bilateral (n=3); multiple sclerosis (n=1). Also, our sample contained only one patient with transcortical motor aphasia; this patient had to be excluded because, in our study, each aphasia type has to be represented by, at the very least, two people (one for training the classifier, and another for testing it). Of the 98 participants whose data constituted the final study sample, 5 aphasia types were observed:

- Anomic aphasia: 35 patients;
- Broca's aphasia: 33 patients;
- Wernicke's aphasia: 7 patients;
- conduction aphasia: 13 patients;
- global aphasia: 10 patients.

Aphasia types were classified according to the Western Aphasia Battery (WAB; Kertesz, 1982; see Supplementary Table 1). The number of patients differed across aphasia types, generally, reflecting the difference in incidence and prevalence of these types of aphasia in the population, but more specifically of those who self-refer for participation in research. The mean sample age was 58 years (standard deviation = 11.9; range = 31–80), and 36 were women. All patients were at least 6 months post-stroke, and the mean time since stroke onset was 40.1 months (SD= 49.6; range = 6–276). Supplementary Table 2 lists the demographic information for each studied patient.

2.2 MRI data collection and preprocessing

MRI scanning was performed within two days of behavioural testing of language abilities. Images were acquired on a Siemens Trio 3T scanner equipped with a 12-element head coil located at the University of South Carolina. These images utilized a T1-weighted MP-RAGE sequence with 1 mm isotropic voxels, a 256×256 matrix size, and a 9-degree flip angle. For the first 25 individuals we used a 160 slice sequence with TR=2250 ms, TI=900 ms, TE=4.52 ms. For the latter 72 individuals, we used a 192 slice sequence with TR=2250 ms, TI=925 ms, TE=4.15 ms with parallel imaging (GRAPPA=2, 80 reference lines). Each of these scans required about 7 minutes to acquire. We also acquired a T2-weighted image

using a sampling perfection with application optimized contrasts using a different flip angle evolution (3D-SPACE) sequence. This 3D TSE scan uses a TR=2800 ms, a TE of 402 ms, variable flip angle, 256×256 matrix scan with 192 1 mm thick slices, using parallel imaging (GRAPPA x2, 120 reference lines).

Lesions were manually drawn on the T2 weighted image by a trained neurologist. The T2 image was then coregistered to match the T1 image, and these parameters were used to reslice the lesion into the native T1 space. The resliced lesion maps were smoothed with a 3 mm full-width half maximum Gaussian kernel to remove jagged edges associated with manual drawing. We then performed enantiomorphic normalization (Nachev et al., 2008) using SPM12 and Matlab scripts we developed. The enantiomorphic normalization steps were as follows. First, a mirrored image of the T1 scan (reflected around the longitudinal fissure) was created, and this mirrored image was coregistered to the native T1 image. We then created a chimeric image based on the native T1 scan with the lesioned tissue replaced by tissue from the mirrored scan (using the smoothed lesion map to modulate this blending, feathering the lesion edge). SPM12's unified segmentation-normalization (Ashburner & Friston, 2005) was used to warp this chimeric image to standard space, with the resulting spatial transform applied to the actual T1 scan as well as the lesion map. The normalized lesion map was then binarized using a 50% probability threshold. Figure 1 shows the overlap of lesions for patients of each aphasia type.

2.3 Segmentation

To segment the brain and compute the damage to each brain area, we used five different atlases:

1. Speculative ***Brodmann*** atlas; 82 areas (provided by Professor Krish Singh of Cardiff University)
2. An atlas containing both grey and white matter developed by Faria et al., (2012), which we refer to as John Hopkins University (***JHU***) atlas; 189 areas
3. ***AAL*** atlas: 116 grey-matter areas (Tzourio-Mazoyer et al., 2001)
4. An atlas of white-matter tracts (Catani & Thiebaut de Schotten, 2008), which we refer to as CTS (Catani - Thiebaut de Schotten) atlas for the sake of brevity; 34 areas
5. A union of AAL and CTS atlases (***AALCTS***); 150 areas. This novel atlas was made by combining the AAL and CTS atlases (in cases of spatial overlap between the atlases, we used the labels from the CTS atlas)

We decided to use Brodmann's atlas for its historical importance in behavioural neuroscience and neurology, and the AAL atlas for its popularity in the field (according to Google Scholar, the paper by Tzourio-Mazoyer et al., 2001 has been referenced more than 5,000 times). The CTS atlas was selected because it is well-established in the field (it has been cited more than 500 times according to Google Scholar), and because it has been developed for a general, not age-specific population. Compared to these atlases, the JHU atlas is relatively new; it was created using a more powerful MRI scanner (3T compared to

1.5T used in Catani & Thiebaut de Schotten, 2008), and Tzourio-Mazoyer et al., 2001) and a larger sample of patients (20 patients; in contrast, 12 patients were used by CTS et al., and a single patient was used by Tzourio-Mazoyer et al., 2001); the authors (Faria et al., 2012) have extensively evaluated its across-subject reproducibility and applicability to different modalities (anatomical and functional MRI and DTI).

Supplementary Table 3 lists the names of the brain areas used in each atlas. Since damage was constrained to the left hemisphere, right-hemisphere areas were excluded from the analysis. Furthermore, areas that were not damaged in any patients were excluded as well. For the remaining areas, we computed the percentage of damage as the ratio of lesioned voxels to the total number of voxels in the area.

2.4 Classification

Support vector machines (SVMs) were used to predict the aphasia type from brain damage. The percentage of damage to the brain areas served as the input to a classifier, and the aphasia type was the output. We used the implementation provided by LIBSVM Matlab library (Chang & Lin, 2011). We used the radial-basis-function kernel, which is the default in LIBSVM (the kernel width was set to its default level, which is 1/number of features). The penalty parameter C was optimized (during training, we ran the classification using different values of C, to determine the optimal value). Aphasia type was predicted in a series of binary (two-class) problems; for 5 aphasia types, there are 10 ways of pairing one type versus another. In addition, we ran a multi-class classification, where all 5 aphasia types were used in one classification problem.

2.5 Training and testing the classifier

The different patient groups, representing different aphasia types, were not balanced in size. If we used the leave-one-out procedure, the groups would be represented with a different number of training examples, and this could bias the classification towards larger groups (Pereira et al., 2009). Overall average classification accuracy might be well above chance because test examples from larger groups would be classified accurately, but this would be at the expense of inaccurate prediction for the smaller group. To avoid this bias, we used a resampling procedure whereby the classes were represented with the same number of training examples. At each resampling iteration, one patient from the smaller group was held out, and the remaining patients were used for training. In the larger group, the number of training examples was the same as for the smaller group, and the remaining patients were used for testing. For example, we have 30 patients with anomic aphasia, and only 9 patients with global aphasia. To train the classifier, we randomly select 8 patients with global aphasia, and the same number of patients with anomic aphasia; our test set is composed of one patient with global aphasia, and 22 patients with anomic aphasia. Because the groups are balanced during training, there is no bias toward either group.

This resampling procedure was done repeatedly, creating a unique training-test split at each repetition. If the size of the larger group is N and the size of the smaller group is M, there are unique training-test splits. The resampling procedure was repeated either N_{splits} or 500

times, whichever number was smaller. At each iteration, we checked the uniqueness of the training-test splits by making sure this split had not been used before.

During training, we performed another round of cross-validation to determine the optimal value for the *C* (penalty) parameter. This was done with 8-fold cross-validation: the training set was separated into 8 subsets of roughly equal size (the difference in size between any two subsets was at most 1 patient). We tested 10 different values for *C* (0.0001, 0.001, 0.01, 0.1, 1, 2, 10, 100, 1000, 10000). For each tested value, we iterated 8 times: one subset was held out to test the classifier, and the remaining 7 subsets were merged and used for training with a specific setting of *C*. Thus, we computed the average classification accuracy for each value of *C*, and identified the value that optimized the accuracy. This value of *C* was then used to classify the test set (which was disjoint from the training set, in order to prevent overfitting).

2.6 Evaluation of significance

When group sizes are unequal, one could suggest two levels for 'chance' performance: either 50% (as there are two choices) or the more stringent incidence of the more frequent class. We chose the latter. For example, consider a symptom present in 80% of the population. In this case, one can perform at 80% classification accuracy by simply guessing that everyone has the symptom. Given this, significance of test-set classification accuracy was evaluated with a binomial distribution (Pereira et al., 2009). Let us consider a two-class problem with classes of size *N* and *M* (where $N \geq M$); we want to know whether the observed classification accuracy is better than chance. Because of unbalanced group sizes, a classifier operating at chance level assigns the test example to the larger group with $N/(N+M)$ frequency, and to the smaller group with $M/(N+M)$ frequency. The probability of correctly guessing *k* test examples out of *n* is given by the density function of the binomial distribution (Freund & Walpole, 1980):

$$f(k;n,p)=\begin{pmatrix} n \\ k \end{pmatrix} p^k(1-p)^{n-k}, \quad (1)$$

where $p= N/(N+M)$. The *p* value (the probability of obtaining at least *k* successes out of *n* trials under the null hypothesis of the classifier operating at chance) is $P(X \geq k)$, where *X* is a binomial random variable with distribution defined by (1). To compute these *p* values for the observed classification accuracy *y*, we used $n=500$ and $k=500*y$ (in practice, any large number could be used for *n* because *y* was an accurate estimate of classification accuracy obtained on a large number of training-test splits). False discovery rate (Genovese et al., 2002) was used to correct for multiple comparisons.

2.7 Classification maps

For binary classification, we created brain maps where the loading on each brain area reflected its importance in classification. In the case of a linear classifier, these loadings are given by the angle of the hyperplane that separates the two classes (see Kjems et al., 2002 for a general discussion, and LaConte et al., 2005 for application to SVM). Since our number of features (brain areas) is large relative to the number of training examples, radial

basis function (RBF) kernel is approximately equivalent to linear kernel with an adjusted penalty parameter (Keerthi & Lin, 2003). Therefore, the brain loadings can be approximated using a weighted product of support vectors:

$$\mathbf{w}=\sum_{i=1}^{N_{sv}} c_i \mathbf{x}_i, \quad (2)$$

where N_{sv} is the number of support vectors, and $\mathbf{x}_i$ and c_i are the support vectors and their associated coefficients, computed by LIBSVM for a particular training set. The *j*th element of **w** is the loading for the *j*th brain area. The absolute value of the loading indicates the relevance of this brain area to aphasia type prediction, and the sign of the loading indicates the "preference" of the area; for a particular two-class contrast, the area has a preference for a given class if larger damage to this area increases the chance of the patient to be assigned to that class (Rasmussen et al., 2012; Yourganov et al., 2014).

When classifying a particular contrast, we computed the brain loadings for each training-test split, computed the mean loading of each area across splits, and normalized the loading by dividing by the standard deviation of the loadings of this area across splits. In addition, for each aphasia type, we computed the *predictive relevance* of each brain area, which indicated the relevance of this brain area in distinguishing a particular aphasia type from all other types. To compute the predictive relevance, we calculated the normalized brain loadings for all pairings of the particular aphasia type with the other 4 aphasia types. Then, we identified the areas that had positive loadings (that is, increased damage to these areas would increase the chance of the patient to be categorized as having the particular aphasia type), and computed the weighted average of these positive loadings across 4 pairings of aphasia types. The weights were the ratios of the number of patients in the contrasted aphasia type to the total number of patients. The purpose of the weighting was to give more influence to the pairings of aphasia groups with greater number of patients because these groups are more representative of the general patient population.

3. RESULTS

The accuracy of predicting the aphasia type is summarized in Tables 1 and 2 and Supplementary Table 4. The prediction was framed as a two-class problem (i.e., we tried to differentiate between two aphasia types). Table 1 lists the accuracy of predicting one aphasia type versus another, that is, the ratio of patients with aphasia type correctly predicted. Table 2 lists, for each pairing of types, the prediction accuracy per each class (this would be analogous to sensitivity/specificity if the two classes were defined according to presence/absence of a symptom). Supplementary Table 4 lists the values of balanced accuracy for each contrast (computed as the average of the two per-class accuracies). Our sample contained patients with 5 aphasia types, which yielded 10 pairings of classes. For each pairing, we trained the classifier on the damage to brain areas defined using 5 different brain atlases. The accuracies that are significantly better than chance (after correcting for multiple comparisons controlling the false discovery rate) are noted with asterisks in Tables 1 and 2. There was a pronounced difference in the number of patients per aphasia type; because of this, some seemingly high accuracies are not significantly better than chance. For example,

the prediction of anomic versus Wernicke's aphasia (represented with 35 and 7 patients, respectively) was never significantly better than chance, regardless of brain atlas used to define the brain areas. For this contrast, the most accurate prediction (81.28%) was obtained with the CTS atlas; however, if we simply assumed that a patient has anomic aphasia without looking at the underlying brain damage, we would be accurate 35/(35+7)=83.33% percent of the time.

Overall, the AALCTS atlas was the most successful: it could resolve 7 out of 10 contrasts. The JHU atlas could resolve 5 contrasts, and the other atlases could resolve 6 contrasts. The average performance of AALCTS was the highest, and the average performance of the CTS white-matter atlas was the lowest; however, the differences in classification accuracy between atlases were not significant (Friedman test for column effects: $p = 0.355$; Wilcoxon signed-rank test between CTS and AALCTS atlases: $p = 0.106$). AALCTS was the only atlas that could successfully classify Broca's versus Wernicke's aphasia. Three contrasts could not be resolved using any atlas: anomic versus Wernicke's, Broca's versus global, and conduction versus Wernicke's aphasia.

Figures 2 and 3 illustrate the importance of various brain areas (defined with AALCTS) to two-class prediction of aphasia type. For each pairing of aphasia types, we computed the loading of each brain area that indicated its contribution to classification. The sign of the loading indicated the aphasia-type preference of the area. Formally speaking, a preference of area X for aphasia type Y means that increased damage to the area X in a random patient would increase the chance of assigning this patient to aphasia type Y. The loadings presented in Figures 2 and 3 are normalized (each loading is divided by the standard deviation across all loadings for a given contrast). The maps are not thresholded.

Each row in Figures 2 and 3 represent a contrast of one aphasia type ("type #1") versus another ("type #2"). For example in the bottom row of Figure 2, type #1 is Broca's aphasia and type #2 is conduction aphasia. Areas shown in blue and green have preference for Broca's aphasia, with green areas being the most relevant and blue being least relevant to classification. Similarly, yellow areas are most relevant with preference for conduction aphasia, and red areas are the least relevant.

Examining the brain area loadings on Figure 2, we see that no brain areas are strongly predictive of anomic aphasia in our set of patients. Although anomic aphasia can be easily distinguished from most other aphasia types (Table 1), there appears to be no spatial pattern of brain damage specific for anomic aphasia (and distinguishing it from *all* other aphasia types). However, all other aphasia types have stronger associations with particular brain areas. Table 3 lists the brain areas for each of these aphasia types. The number alongside each area is its predictive relevance, computed as a weighted average of *Z*-scores across pairings of aphasia types (see section 2.7; a higher value indicates a more relevant area). Areas with predictive relevance less than 1 are not listed. Figure 4 shows the corresponding brain maps where the colour of each brain area indicates the predictive relevance for a particular aphasia type (again, only areas with predictive relevance of at least 1 are displayed).

As shown in Table 3 and Figure 4 (top row), Broca's aphasia is strongly associated with damage to pars opercularis of the inferior frontal gyrus, corresponding to Brodmann area 44 and generally considered a part of Broca's area. Its posterior neighbour, rolandic operculum, also has high predictive relevance. The most relevant white-matter tract is the arcuate fasciculus, particularly the long and anterior segments. Conduction aphasia is associated with damage to the posterior segment of the arcuate fasciculus, Heschl's gyrus, and optical tracts. Global aphasia is associated with extensive cortical damage. Middle and inferior frontal gyri, temporal regions (temporal pole; Heschl's and superior temporal gyri), insula and rolandic operculum, pre- and postcentral gyri, and putamen all had high predictive relevance for global aphasia. Among the white-matter tracts, uncinate and arcuate fasciculi, particularly the long and anterior segments of the latter, were also found to be predictive of global aphasia. Finally, Wernicke's aphasia can be predicted from damage to angular, Heschl's, and superior temporal gyri, as well as temporal pole and putamen.

4. DISCUSSION

We have demonstrated that the aphasia types found in our sample (Broca's, Wernicke's, conduction, global, and anomic) could be, in most cases, distinguished from each other on the basis of damage to atlas-defined brain areas. In particular, the fluent aphasia types (Wernicke's, conduction, and anomic aphasia) could be distinguished from non-fluent types (Broca's and global aphasia), if the novel AALCTS atlas was used to define the brain areas. The classification accuracy for the pairings of fluent versus non-fluent types was 87% and higher, and was significantly above chance for all such pairings. We had less success with pairings of fluent aphasia types: of the three such pairings, only conduction versus anomic aphasia could be resolved at a level of accuracy significantly better than chance. Also, the classification accuracy for the pairing of the two non-fluent aphasia types (global versus Broca's aphasia) was at chance level. This poor result could be driven by the similarity in the patterns of brain damage in non-fluent aphasia (see Figure 1, second and fourth row). Also, if we look at the areas that are predictive of Broca's and global aphasia (Table 3), we see that the vast majority of the brain areas that are predictive of Broca's aphasia are also predictive of global aphasia. Finally, global aphasia often resolves into Broca's aphasia (Pedersen, 2003), indicating that, for some patients, we are perhaps dealing with two stages of the same process rather than two phenomenologically different neurological conditions.

The areas where the damage is predictive of the aphasia type (listed in Table 3) are largely consistent with the previous aphasia research (see, for example, reviews by Damasio, 1992; Marshall et al., 1998; and chapter 2 in Davis, 2007). We found that Broca's aphasia could be predicted from damage to pars opercularis, adjacent white-matter tracts, and globus pallidus. Damage to these areas has previously been reported as critical lesion locations associated with Broca's aphasia; moreover, Broca's aphasia is not present when damage is limited to Broca's area or to the basal ganglia (Damasio, 1992; Alexander et al., 1987, Mohr et al., 1978). In addition, we found that damage to supramarginal and Heschl's gyri predicts Broca's aphasia, consistent with Fridriksson et al. (2014).

The group of patients with Wernicke's aphasia was the smallest (n=7) patient group in our sample. Despite the sample size limitation, the brain areas that we found to predict

Wernicke's aphasia include the classical Wernicke's area and its neighbourhood, which is consistent with the existing literature (Marshall et al., 1998; Lieberman, 2002). In addition, the damage to the temporal poles and the putamen was also associated with Wernicke's aphasia, which may reflect the idiosyncrasies of our small sample (see the lesion overlay map in Figure 1). Conduction aphasia is thought to be linked to damage of regions in the neighbourhood of temporo-parietal junction (Damasio, 1992; Hickok et al., 2000; Dick & Tremblay, 2012). Our results are consistent with this picture: in our sample, conduction aphasia is associated with damage to Heschl's gyrus and the adjacent white-matter tracts (posterior segment of the arcuate fasciculus; optic radiations). Global aphasia is the most severe form of aphasia, and has long been associated with extensive cortical damage in the region supplied by the middle cerebral artery. Consistent with previous reports (Damasio, 1992; Marshall et al., 1998), we have found this type of aphasia to be associated with damage to areas predictive for Broca's and Wernicke's aphasia, as well as insular regions. Finally, anomic aphasia, the least severe of aphasia types, could be easily distinguished, but no brain areas were found to be strongly predictive (a similar result was reported in a voxel-based lesion symptoms mapping study of Henseler et al., 2014).

We achieved the numerically best prediction accuracy with the novel AALCTS atlas, which includes both grey and white matter areas. Interestingly, the CTS atlas, composed solely of white-matter tracts, provided reasonably effective features for aphasia-type prediction, and predicted aphasia type above chance in 6 out of 10 pairings of aphasia types. This suggests that the behavioural deficiencies captured by the WAB scores are to some extent driven by damage to white matter tracts. A similar level of accuracy was achieved with the Brodmann atlas; however, we do not recommend this parcellation because it does not include some areas that are predictive of aphasia type, such as the insula and basal ganglia.

Traditional classifications of the aphasia syndromes emerged due to the clinically observed consistency of patterns of language impairment related to lesions of specific locations. Although many variations of classifications systems have been proposed over several years, the descriptions of language disorders clustered as syndromes and anatomical substrates have remained relatively stable since the days of Wernicke and Lichtheim (Benson & Ardila, 1996; Goodglass & Kaplan, 1983). While the validity of aphasia classification systems has been challenged (Caplan, 1993; Wertz et al., 1984), reporting classification type remains common in clinical and research settings. Several problems can be pointed out with using a behavioural battery like the WAB for determining patient's aphasia types. For instance, it is possible that the behavioural assessment might not match the clinical impression. Also, the aphasia type is questionable for a patient whose behavioural score is at the threshold level between two aphasia types (which is particularly problematic for scores that rely on subjective opinion of the clinician completing the assessment). Despite these potential problems, our results suggest that the Western Aphasia Battery provides criteria for consistently classifying aphasia syndromes, some of which can be strongly predicted based on patterns of underlying neural damage.

A next step will be to predict the expected aphasia type and recovery prognosis based on a patient's acute symptoms. Identifying prognosis and potential for recovery is critical, as acute patients and caregivers need to know how their future quality of life might be affected

by the stroke. Some aphasia syndromes are quite resistant to improvement, while others tend to recover more easily (Kertesz & McCabe, 1977; McDermott et al., 1996). For example, acute Broca's aphasia and conduction aphasia sometimes resolve to anomic aphasia, while Wernicke's aphasia may develop into either anomic or conduction aphasia (Pashek & Holland, 1988; Benson & Ardila, 1996). We can predict that classification, using the approach described here, would hold up over the course of recovery; as recovery occurs, the type of aphasia manifested in the chronic stage represents the neuroplasticity associated with recovery. Our results demonstrate that chronic aphasia types can, in fact, be distinguished from each other based on damage to atlas-defined brain areas. Importantly, our findings provide support for both historical and current accounts that associate patterns of brain damage with fairly predictable patterns of speech-language impairment.

Supplementary Material

Refer to Web version on PubMed Central for supplementary material.

Acknowledgments

This research has been supported by the NIH grant (R01 DC009571) to JF and CR.

References

Alexander MP, Naeser MA, Palumbo CL. Correlations of subcortical CT lesion sites and aphasia profiles. Brain. 1987; 110:961–991. [PubMed: 3651803]

Alexander MP, Hiltbrunner B, Fischer RS. Distributed anatomy of transcortical sensory aphasia. Archives of Neurology. 1989; 46(8):885–892. [PubMed: 2757529]

Anderson JM, Gilmore R, Roper S, Crosson B, Bauer RM, Nadeau S, Heilman KM. Conduction aphasia and the arcuate fasciculus: a reexamination of the Wernicke–Geschwind model. Brain and language. 1999; 70(1):1–12. [PubMed: 10534369]

Ardila A. A proposed reinterpretation and reclassification of aphasic syndromes. Aphasiology. 2010; 24(3):363–394.

Ashburner J, Friston KJ. Unified segmentation. Neuroimage. 2005; 26(3):839–851. [PubMed: 15955494]

Basso A, Lecours AR, Moraschini S, Vanier M. Anatomoclinical correlations of the aphasias as defined through computerized tomography: exceptions. Brain and language. 1985; 26(2):201–229. [PubMed: 2417656]

Bates E, Wilson SM, Saygin AP, Dick F, Sereno MI, Knight RT, Dronkers NF. Voxel-based lesion–symptom mapping. Nature neuroscience. 2003; 6(5):448–450. [PubMed: 12704393]

Benson, DF.; Ardila, A. Aphasia: A clinical perspective. New York: Oxford University Press; 1996.

Buchsbaum BR, Baldo J, Okada K, Berman KF, Dronkers N, D'Esposito M, Hickok G. Conduction aphasia, sensory-motor integration, and phonological short-term memory–an aggregate analysis of lesion and fMRI data. Brain and language. 2011; 119(3):119–128. [PubMed: 21256582]

Caplan, D. Neurolinguistics and linguistic aphasiology: An introduction. Cambridge University Press; 1987.

Caplan D. Toward a psycholinguistic approach to acquired neurogenic language disorders. American Journal of Speech-Language Pathology. 1993; 2(1):59–83.

Caramazza A, McCloskey M. The case for single-patient studies. Cognitive Neuropsychology. 1988; 5(5):517–527.

Caramazza A. The logic of neuropsychological research and the problem of patient classification in aphasia. Brain and Language. 1984; 21(1):9–20. [PubMed: 6697172]

Catani M, Thiebaut de Schotten M. A diffusion tensor imaging tractography atlas for virtual in vivo dissections. Cortex. 2008; 44(8):1105–1132. [PubMed: 18619589]

Chang C-C, Lin C-J. LIBSVM : a library for support vector machines. ACM Transactions on Intelligent Systems and Technology. 2011; 2(3):Article # 27.

Chapey, R. Language intervention strategies in aphasia and related neurogenic communication disorders. Lippincott Williams & Wilkins; 2001.

Damasio H, Damasio AR. The anatomical basis of conduction aphasia. Brain. 1980; 103:337–350. [PubMed: 7397481]

Damasio AR. Aphasia. New England Journal of Medicine. 1992; 326(8):531–539. [PubMed: 1732792]

Davis, GA. Aphasiology: Disorders and clinical practice. Pearson College Division; 2007.

Dick AS, Tremblay P. Beyond the arcuate fasciculus: consensus and controversy in the connectional anatomy of language. Brain. 2012; 135(12):3529–3550. [PubMed: 23107648]

Faria AV, Joel SE, Zhang Y, Oishi K, van Zjil P, Miller MI, Pekar JJ, Mori S. Atlas-based analysis of resting-state functional connectivity: Evaluation for reproducibility and multi-modal anatomy–function correlation studies. Neuroimage. 2012; 61(3):613–621. [PubMed: 22498656]

Freedman M, Alexander MP, Naeser MA. Anatomic basis of transcortical motor aphasia. Neurology. 1984; 34(4):409–409. [PubMed: 6538298]

Freund, J.; Walpole, R. Mathematical statistics. Engiewood Gliffs, NJ: Prentice-Hall; 1980.

Fridriksson J, Fillmore P, Guo D, Rorden C. Chronic Broca's Aphasia Is Caused by Damage to Broca's and Wernicke's Areas. Cerebral Cortex. 2014:bhu152.

Genovese CR, Lazar NA, Nichols T. Thresholding of statistical maps in functional neuroimaging using the false discovery rate. Neuroimage. 2002; 15(4):870–878. [PubMed: 11906227]

Geschwind N, Kaplan E. A human cerebral deconnection syndrome. Neurology. 1962; 12(10):675–685. [PubMed: 13898109]

Geschwind N. Disconnexion syndromes in animals and man. Brain. 1965; 88(3):585–644. [PubMed: 5318824]

Geschwind N, Fusillo M. Color-naming defects in association with alexia. Archives of Neurology. 1966; 15(2):137–146. [PubMed: 5945970]

Goodglass, H.; Kaplan, E. Boston Diagnostic Aphasia Examination (BDAE). Philadelphia: Lea & Febiger; Psychological Assessment Resources; Odessa, FL: 1983.

Hastie, T.; Tibshirani, R.; Friedman, J. The elements of statistical learning. New York: Springer; 2009.

Henseler I, Regenbrecht F, Obrig H. Lesion correlates of patholinguistic profiles in chronic aphasia: comparisons of syndrome-, modality-and symptom-level assessment. Brain. 2014; 137:918–930. [PubMed: 24525451]

Hickok G, Erhard P, Kassubek J, Helms-Tillery AK, Naeve-Velguth S, Strupp JP, Strick PL, Ugurbil K. A functional magnetic resonance imaging study of the role of left posterior superior temporal gyrus in speech production: implications for the explanation of conduction aphasia. Neuroscience letters. 2000; 287(2):156–160. [PubMed: 10854735]

Hillis AE. Aphasia Progress in the last quarter of a century. Neurology. 2007; 69(2):200–213. [PubMed: 17620554]

Keerthi SS, Lin CJ. Asymptotic behaviors of support vector machines with Gaussian kernel. Neural computation. 2003; 15(7):1667–1689. [PubMed: 12816571]

Kertesz A, McCabe P. Recovery patterns and prognosis in aphasia. Brain. 1977; 100:1–18. [PubMed: 861709]

Kertesz, A. Western aphasia battery test manual. Psychological Corp; 1982.

Kertesz, A. Recovery of aphasia. In: Feinberg, TE.; Farah, MJ., editors. Behavioral neurology and neuropsychology. New York: McGraw Hill; 1997. p. 167-182.

Kertesz, A. Western Aphasia Battery–Revised (WAB-R). Pearson; San Antonio: 2006.

Kjems U, Hansen LK, Anderson J, Frutiger S, Muley S, Sidtis J, Rotenber D, Strother SC. The quantitative evaluation of functional neuroimaging experiments: Mutual information learning curves. NeuroImage. 2002; 15(4):772–786. [PubMed: 11906219]

Kreisler A, Godefroy O, Delmaire C, Debachy B, Leclercq M, Pruvo JP, Leys D. The anatomy of aphasia revisited. Neurology. 2000; 54(5):1117–1123. [PubMed: 10720284]

LaConte S, Strother S, Cherkassky V, Anderson J, Hu X. Support vector machines for temporal classification of block design fMRI data. NeuroImage. 2005; 26(2):317–329. [PubMed: 15907293]

Lichteim L. On aphasia. Brain. 1885; 7(4):433–484.

Lieberman P. On the nature and evolution of the neural bases of human language. American Journal of Physical Anthropology. 2002; 119(S35):36–62. [PubMed: 12653308]

Luria, AR. Traumatic aphasia: Its syndromes, psychology and treatment. Vol. 5. Walter De Gruyter; 1970.

Mah YH, Husain M, Rees G, Nachev P. Human brain lesion-deficit inference remapped. Brain: a journal of neurology. 2014; 137(9):2522–2531. [PubMed: 24974384]

Marshall RS, Lazar RM, Mohr JP. Aphasia. Medical Update for Psychiatrists. 1998; 3(5):132–138.

Masdeu JC, Schoene WC, Funkenstein H. Aphasia following infarction of the left supplementary motor area. Neurology. 1978; 28(12):1220–1220. [PubMed: 569781]

Mazzocchi F, Vignolo LA. Localisation of lesions in aphasia: clinical-CT scan correlations in stroke patients. Cortex. 1979; 15(4):627–653. [PubMed: 95004]

Mohr JP, Pessin MS, Finkelstein S, Funkenstein HH, Duncan GW, Davis KR. Broca aphasia: Pathologic and clinical. Neurology. 1978; 28(4):311–311. [PubMed: 565019]

Nachev P, Coulthard E, Jäger HR, Kennard C, Husain M. Enantiomorphic normalization of focally lesioned brains. NeuroImage. 2008; 39(3):1215–1226. [PubMed: 18023365]

Orrù G, Pettersson-Yeo W, Marquand AF, Sartori G, Mechelli A. Using support vector machine to identify imaging biomarkers of neurological and psychiatric disease: a critical review. Neuroscience & Biobehavioral Reviews. 2012; 36(4):1140–1152. [PubMed: 22305994]

Palumbo, CL.; Alexander, MP.; Naeser, MA. CT scan lesion sites associated with conduction aphasia. In: Kohn, SE., editor. Conduction aphasia. Hillsdale: Lawrence Erlbaum; 1992. p. 51-75.

Pashek GV, Holland AL. Evolution of aphasia in the first year post-onset. Cortex. 1988; 24(3):411–423. [PubMed: 3191724]

Pedersen P, Vinter K, Olsen TSOJ. Aphasia after stroke: type, severity and prognosis. Cerebrovascular Diseases. 2003; 17(1):35–43. [PubMed: 14530636]

Pereira F, Mitchell T, Botvinick M. Machine learning classifiers and fMRI: a tutorial overview. Neuroimage. 2009; 45(1):S199–S209. [PubMed: 19070668]

Rasmussen, PM.; Schmah, T.; Madsen, KH.; Lund, TE.; Yourganov, G.; Strother, S.; Hansen, LK. Visualization of nonlinear classification models in neuroimaging— signed sensitivity maps. Paper presented at the Biosignals 2012, International Conference on Bio-inspired Systems and Signal Processing; 2012.

Reineck LA, Hillis AE. “Diffusion-Clinical Mismatch” predicts potential for early recovery of aphasia. Stroke. 2004; 35:287.

Reineck LA, Agarwal S, Hillis AE. “Diffusion-clinical mismatch” is associated with potential for early recovery of aphasia. Neurology. 2005; 64(5):828–833. [PubMed: 15753418]

Rorden C, Bonilha L, Fridriksson J, Bender B, Karnath HO. Age-specific CT and MRI templates for spatial normalization. Neuroimage. 2012; 61(4):957–965. [PubMed: 22440645]

Rubens, AB. Transcortical motor aphasia. In: Whitaker, H.; Whitaker, H., editors. Studies in neurolinguistics. New York: Academic; 1976. p. 293-306.

Saur D, Ronneberger O, Kümmerer D, Mader I, Weiller C, Klöppel S. Early functional magnetic resonance imaging activations predict language outcome after stroke. Brain. 2010; 133(4):1252–1264. [PubMed: 20299389]

Schmah T, Yourganov G, Zemel RS, Hinton GE, Small SL, Strother SC. Comparing classification methods for longitudinal fMRI studies. Neural computation. 2010; 22(11):2729–2762. [PubMed: 20804386]

Schwartz MF. What the classical aphasia categories can’t do for us, and why. Brain and Language. 1984; 21(1):3–8. [PubMed: 6697169]

Selnes OA, van Zijl PC, Barker PB, Hillis AE, Mori S. MR diffusion tensor imaging documented arcuate fasciculus lesion in a patient with normal repetition performance. Aphasiology. 2002; 16(9):897–902.

Smith DV, Clithero JA, Rorden C, Karnath HO. Decoding the anatomical network of spatial attention. Proc Natl Acad Sci U S A. 2013; 110(4):1518–23. [PubMed: 23300283]

Tesak, J.; Code, C. Milestones in the history of aphasia: theories and protagonists. Psychology Press; 2008.

Tzourio-Mazoyer N, Landeau B, Papathanassiou D, Crivello F, Etard O, Delcroix N, Mazoyer B, Joliot M. Automated anatomical labeling of activations in SPM using a macroscopic anatomical parcellation of the MNI MRI single-subject brain. Neuroimage. 2002; 15(1):273–289. [PubMed: 11771995]

Willmes K, Poeck K. To what extent can aphasic syndromes be localized? Brain. 1993; 116(6):1527–1540. [PubMed: 8293285]

Yourganov G, Schmah T, Churchill NW, Berman MG, Grady CL, Strother SC. Pattern classification of fMRI data: Applications for analysis of spatially distributed cortical networks. NeuroImage. 2014; 96:117–132. [PubMed: 24705202]

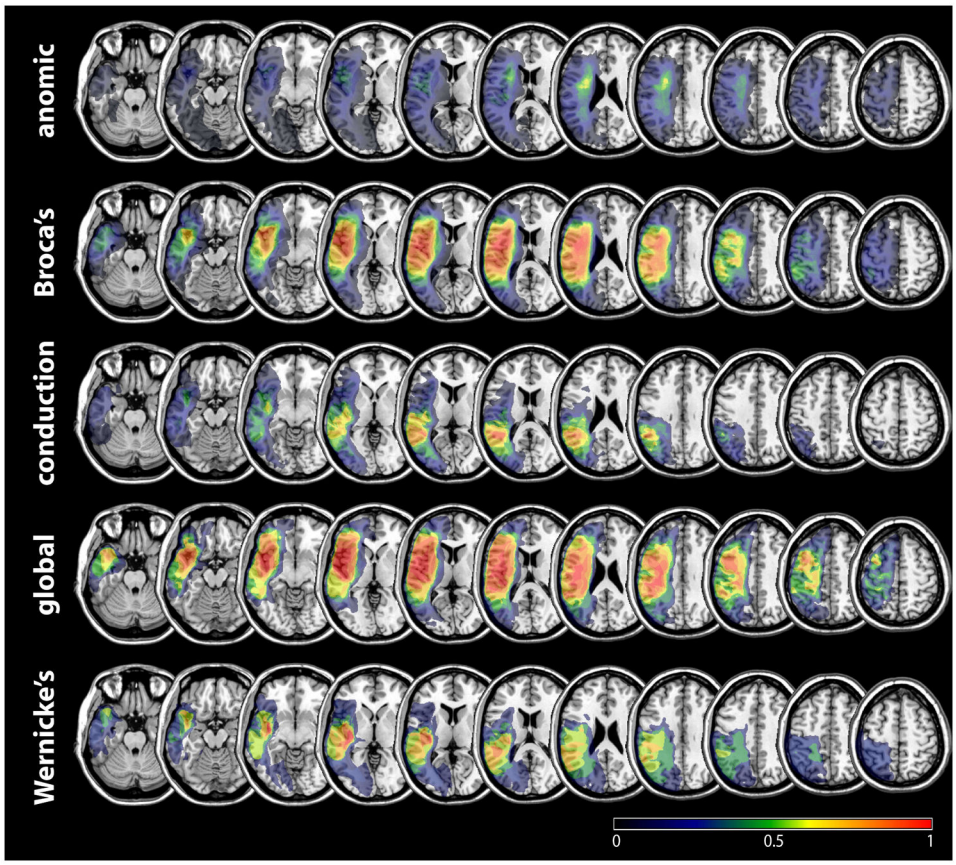

Figure 1.

Overlap of lesions across patients of each aphasia type. A voxel with overlap = 1 indicates that this voxel is lesioned in 100% of the patients.

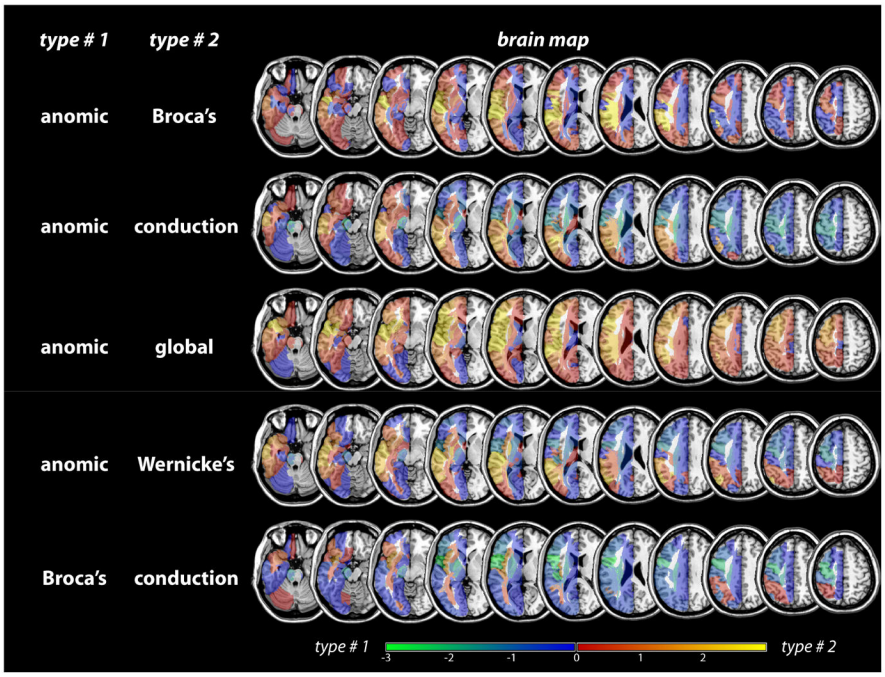

Figure 2.

Brain loadings computed from predicting one aphasia type versus another. See Figure 3 for the remaining 5 pairings of aphasia types.

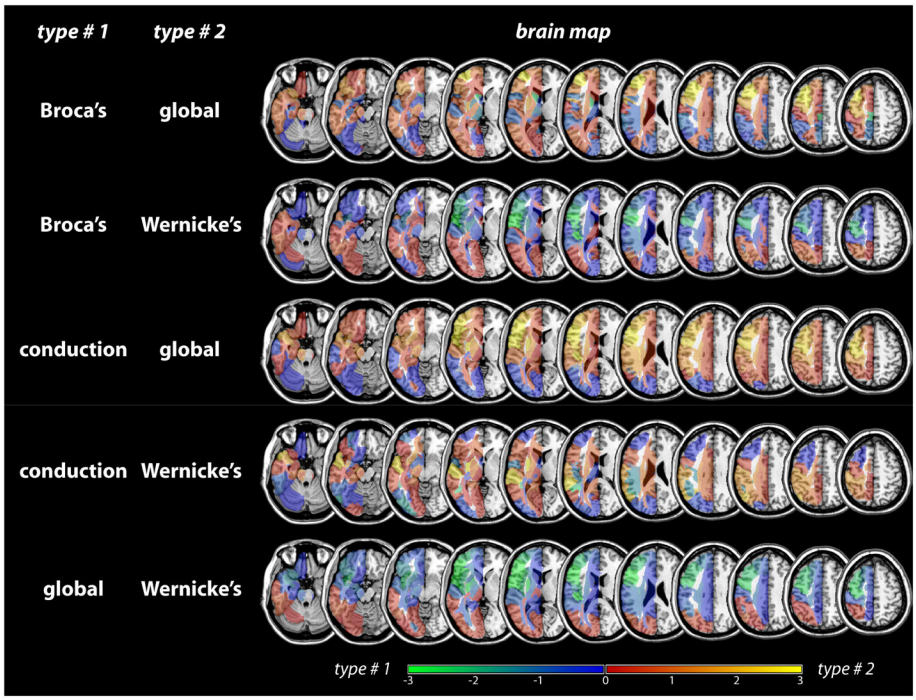

Figure 3.

Brain loadings computed from predicting one aphasia type versus another. See Figure 2 for the remaining 5 pairings of aphasia types.

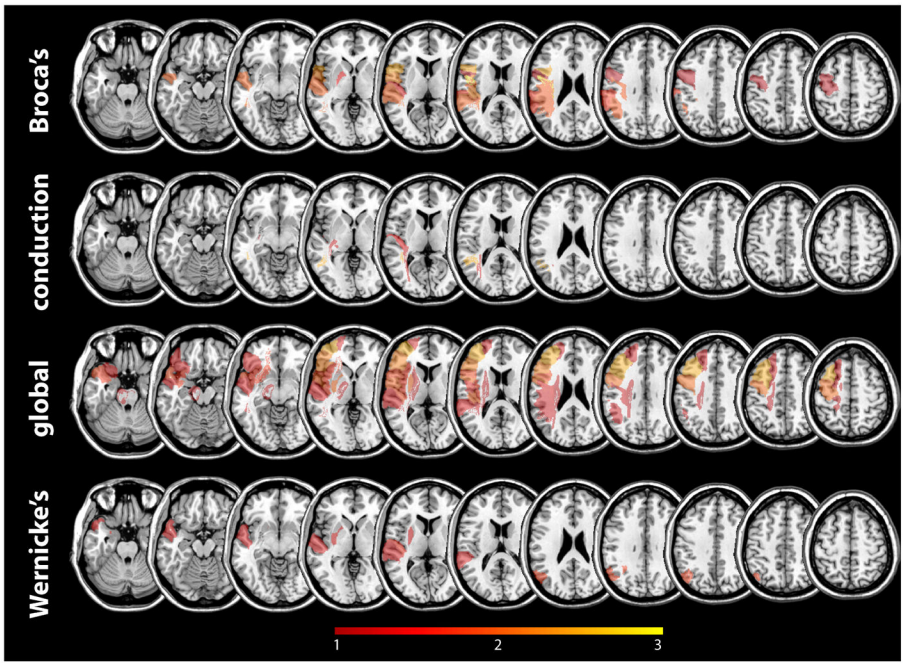

Figure 4.

Areas that are most predictive of each aphasia type (see Table 3) mapped onto a standard brain template. The colour indicates the predictive relevance of a brain area (red being the least predictive, and yellow being the most predictive).

Table 1

Accuracy of aphasia type prediction (given as ratio of patients with aphasia type predicted correctly) for each pairing of aphasia types. Five different atlases were used to define brain areas; the proportional damage to the brain areas comprised the input to the classifier.

contrast	***atlas***					***chance***
	Brodmann	**JHU**	**AAL**	**CTS**	**AALCTS**	
anomic / Broca's	0.8475**	0.8861**	0.8903**	0.8491**	0.8832**	*0.5147*
anomic / conduction	0.8247**	0.7989**	0.7805	0.8294**	0.7965*	*0.7292*
anomic / global	0.9133**	0.9236**	0.9479**	0.8577**	0.9457**	*0.7778*
anomic / Wernicke's	0.7524	0.7712	0.8128	0.7004	0.7807	*0.8333*
Broca's / conduction	0.8277**	0.8906**	0.8674**	0.8585**	0.9356**	*0.7174*
Broca's / global	0.5975	0.5436	0.5818	0.5764	0.5568	*0.7674*
Broca's / Wernicke's	0.7845	0.7766	0.8532	0.8338	0.8787**	*0.825*
conduction / global	0.9541**	0.9204**	0.923**	0.8292**	0.9512**	*0.5652*
conduction / Wernicke's	0.5394	0.5545	0.5031	0.6063	0.5143	*0.65*
global / Wernicke's	0.9104**	0.9139**	0.9373**	0.7585**	0.9198**	*0.5882*

The last column lists the accuracy of chance, in italics (estimated as the size of the larger group divided by the size of both groups combined). Asterisks indicate accuracies that are significantly better than chance, as estimated with binomial distribution (single asterisk: $p<0.05$; double asterisk: $p<0.01$; false discovery rate correction for multiple comparisons).

Table 2

Accuracy of classifying one aphasia type versus another, reported separately for each type (the first type followed by the second type).

	atlas				
contrast	**Brodmann**	**JHU**	**AAL**	**CTS**	**AALCTS**
anomic / Broca's	0.8246** / 0.8739**	0.8596** / 0.9101**	0.8766** / 0.9043**	0.8749** / 0.8503**	0.8752** / 0.8896**
anomic / conduction	0.8482** / 0.8047**	0.8511** / 0.7623	0.8067** / 0.7596	0.9215** / 0.7957**	0.8698** / 0.7699*
anomic / global	0.8789** / 0.9238**	0.8736** / 0.9354**	0.9786** / 0.937**	0.7809 / 0.8751**	0.9898** / 0.9325**
anomic / Wernicke's	0.5908 / 0.789	0.6765 / 0.791	0.7034 / 0.8166	0.5798 / 0.7225	0.6463 / 0.8095
Broca's / conduction	0.8547** / 0.8209**	0.96** / 0.869**	0.8751** / 0.8693**	0.7533 / 0.9053**	0.9591** / 0.9268**
Broca's / global	0.5526 / 0.5893	0.5961 / 0.5123	0.6268 / 0.5696	0.5511 / 0.5749	0.6299 / 0.5333
Broca's / Wernicke's	0.7755 / 0.7813	0.8549 / 0.7666	0.9432** / 0.8409	0.6892 / 0.8725*	0.8737** / 0.8782**
conduction / global	0.9** / 0.9946**	0.9208** / 0.9306**	0.9486** / 0.9094**	0.8923** / 0.7772**	0.9704** / 0.9328**
conduction / Wernicke's	0.3186 / 0.6782	0.3803 / 0.6057	0.3972 / 0.5632	0.5486 / 0.6309	0.3829 / 0.5868
global / Wernicke's	0.9276** / 0.8956**	1** / 0.8499**	0.9706** / 0.9076**	0.7084** / 0.803**	0.9194** / 0.9162**

Asterisks indicate accuracies that are significantly better than chance, as estimated with binomial distribution (single asterisk: $p<0.05$; double asterisk: $p<0.01$; false discovery rate correction for multiple comparisons).

Table 3

Brain areas that are predictive of each aphasia type, with overall predictive relevance given in parentheses. Only areas with predictive relevance > 1 are listed (no such areas were found for anomic aphasia). White-matter tracts are given in italics.

Broca's aphasia	**Conduction aphasia**	**Global aphasia**	**Wernicke's aphasia**
Anterior Segment (3.2)	*Posterior Segment* (2.48)	Middle frontal gyrus (2.51)	Angular gyrus (1.76)
Long Segment (2.85)	Heschl's gyrus (1.47)	Inferior frontal gyrus, triangular (2.18)	Heschl's gyrus (1.61)
Inferior frontal gyrus, opercular (2.45)	*Optic Radiations* (1.14)	Temporal pole: mid. temporal gyrus (2.15)	Temporal pole: mid. temporal gyrus (1.47)
Rolandic operculum (2.2)		Precentral gyrus (2.05)	Temporal pole: sup. temporal gyrus (1.34)
Superior temporal gyrus (1.99)		Putamen (2.02)	Superior temporal gyrus (1.31)
Arcuate (1.91)		Rolandic operculum (1.96)	Putamen (1.3)
Supramarginal gyrus (1.66)		Temporal pole: sup. temporal gyrus (1.81)	
Pallidum (1.45)		Inferior frontal gyrus, opercular (1.78)	
Heschl's gyrus (1.35)		Heschl's gyrus (1.78)	
Precentral gyrus (1.06)		*Uncinate* (1.71)	
		Insula (1.66)	
		Anterior Segment (1.65)	
		Long Segment (1.47)	
		Superior temporal gyrus (1.31)	
		Inferior frontal gyrus, orbital (1.28)	
		Arcuate (1.21)	
		Superior frontal gyrus (1.21)	
		Cortico-Spinal Tract (1.08)	